

# Fluctuation Amplitude of a Trapped Rigid Sphere Immersed in a Near-Critical Binary Fluid Mixture

Youhei Fujitani\*

*School of Fundamental Science and Technology, Keio University, Yokohama 223-8522, Japan*

(Dated: October 14, 2015)

The position of a colloidal particle trapped in an external field thermally fluctuates at the equilibrium. As is well known, the ambient fluid is not a simple heat bath and a moving particle appears heavier, which influences the mean square velocity of the particle. When the ambient fluid is a near-critical binary fluid mixture, the profile of the concentration difference does not follow the particle motion totally, which is expected to influence the mean square displacement of the particle. We calculate the influence in a simple case, where a rigid sphere fluctuates with small amplitude, the mixture in the homogeneous phase is near, but not very close to, the critical point, and the particle surface attracts one component weakly. What we calculate is an equal-time correlation, but we utilize the hydrodynamics in the limit of no dissipation to examine the contribution from the ambient fluid. According to our result, the mean square displacement is reduced by the additional stress, including the osmotic pressure, due to the ambient near-criticality combined with the preferential attraction.

PACS numbers: 05.40.-a, 05.70.Jk, 47.57.-s, 82.70.Dd

## I. INTRODUCTION

Suppose a colloidal particle, about 0.1-1  $\mu\text{m}$  in size, trapped by the optical tweezers. The particle position fluctuates at the equilibrium, which is experimentally observed with high resolutions of space ( $< 1\text{ nm}$ ) and time ( $< 1\text{ }\mu\text{s}$ ) [1–4]. For simplicity, we assume the one-dimensional motion of a rigid sphere (mass  $m$ ) trapped in a harmonic potential (natural angular frequency  $\omega_0$ ) to consider the fluctuation. The positional deviation of the particle center from the potential bottom is denoted by  $\zeta$ , while the equilibrium average at the temperature  $T$  is indicated by  $\langle \cdots \rangle$ . The equal-time correlations can be calculated as

$$\langle \zeta^2 \rangle = \frac{k_B T}{m \omega_0^2} \quad \text{and} \quad \left\langle \left( \frac{d\zeta}{dt} \right)^2 \right\rangle = \frac{k_B T}{m + m_{\text{ind}}} . \quad (1)$$

Here,  $k_B$  denotes the Boltzmann constant, while  $m_{\text{ind}}$  denotes the induced mass, which equals half the displaced mass of the fluid [5]. The ambient fluid cannot be regarded as a heat bath; the particle appears to be heavier because of the fluid part moved by the particle motion. The induced mass can be calculated in terms of the hydrodynamics, *i.e.*, we can detect theoretically how much fluid moves by shaking the particle.

In Eq. (1), the mean square displacement  $\langle \zeta^2 \rangle$  is not influenced by the fluid motion. It is expected not to be the case, however, if the ambient fluid is a near-critical binary fluid mixture. The reason is as follows. It is usual that one component is preferably attracted by the particle surface [6]. Suppose that the correlation length of the mixture is several nanometers, which is much

smaller than the particle radius, and that the ambient fluid is in the homogeneous phase. The adsorption layer, where the preferred component is more concentrated, appears around the particle and has the thickness comparable with the correlation length [7, 8]. The adsorption layer is isotropic when the particle is fixed, as is drawn schematically in Fig. 1(a). There, although the resultant gradient of the concentration difference between the two components generates the osmotic pressure, the total force exerted on the particle by the ambient fluid vanishes. When the particle moves rather rapidly, the adsorption layer cannot follow the motion and is deformed, as shown in Fig. 1(b). Then, the additional force due to the gradient of the concentration difference can be exerted on the particle in total. It is thus possible that the ambient fluid influences the mean square displacement, unlike in Eq. (1). In this paper, we calculate this influence in a simple case. We assume the particle to be neutral electrically and no ion to be involved in the mixture.

We refer to some backgrounds. In this paragraph, without assuming the ambient near-criticality combined with the preferential attraction, we mention the hydrodynamic calculation leading to the induced mass in Eq. (1). The evolution of the particle position  $\zeta$  with respect to the time  $t$  can be described by the Langevin equation [4, 9],

$$m \frac{d^2}{dt^2} \zeta(t) = -m \omega_0^2 \zeta(t) + F_{\text{hy}}(t) + F_{\text{th}}(t) , \quad (2)$$

where  $F_{\text{hy}}$  and  $F_{\text{th}}$  denotes the force exerted by the ambient fluid and the thermal noise, respectively. No particle rotation is assumed. The force  $F_{\text{hy}}$  consists of the term  $-m_{\text{ind}} d^2 \zeta / (dt^2)$ , the term causing the Stokes law, and the term having the memory effect. The latter two terms involves the viscosity. To calculate the equal-time corre-

---

\*Electronic address: youhei@appi.keio.ac.jp

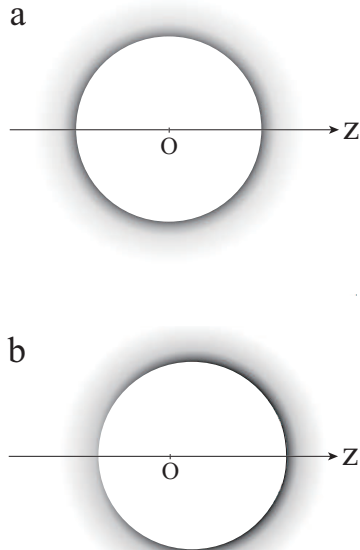


FIG. 1: A cross section of a spherical particle immersed in a near-critical binary fluid mixture is schematically drawn. The gray scale is supposed to reflect the concentration difference between the two components; the dense region represents the adsorption layer. (a) The particle is fixed with its center being located at the origin  $O$ . The adsorption layer is concentric with the particle contour in this figure; the concentration difference is isotropic as viewed from the particle center in practice. (b) At a transient position of the particle in its motion along the  $z$ -axis, the adsorption layer is deformed because the ambient fluid is not shifted translationally.

lation, we need not take into account the dissipation and noise, irrespective of the real dynamics. The reversible part of the dynamics,

$$(m + m_{\text{ind}}) \frac{d^2}{dt^2} \zeta(t) = -m\omega_0^2 \zeta, \quad (3)$$

describes the oscillation about the equilibrium point. From this, we find

$$\frac{1}{2} m\omega_0^2 \zeta^2 + \frac{1}{2} (m + m_{\text{ind}}) \left( \frac{d\zeta}{dt} \right)^2 \quad (4)$$

to give the total energy [10]. Thus, we arrive at Eq. (1) with the aid of the equipartition theorem.

Similarly, we can use the reversible part of the hydrodynamics to calculate the mean square displacement influenced by the deformed adsorption layer, considering that the particle radius is much larger than the correlation length. We can formulate the hydrodynamics by using the free-energy functional renormalized up to the correlation length. It is possible that the resultant

coarse-grained free-energy functional for the bulk is approximately given by the Gaussian model when the mixture in the homogeneous phase is near, but not very close to, the critical point. For details, see Appendix A, where we estimate the temperature range validating the Gaussian model when the mixture has the critical fraction far from the surface. Noting the limitation, we use the Gaussian model. The hydrodynamics formulated from the free-energy functional can be found in the model H, where the dissipation is assumed to study the relaxation of the two-time correlation in a near-critical fluid [17–19]. In the present study, not interested in the critical slowing down, we utilize only the reversible part for calculating the equal-time correlation although the real dynamics is dissipative [11–16].

The preferential attraction is here assumed to be caused by a short-ranged interaction. It is thus represented by the additional free-energy functional determined by the concentration difference immediately near the particle surface. Similar problems were studied in terms of the three-dimensional Ising model in a finite lattice [7, 20–23]. If the coupling between neighboring spins is much stronger at the lattice boundary than in the bulk, the bulk suffers the extraordinary second-order transition in the presence of the spontaneously ordered surface when there is no external field. The normal transition occurs when the surface is ordered by a surface field imposed externally. These two transitions share the same universal properties, and the latter can also be observed in a binary fluid mixture in a container with the preferential attraction. However, these critical phenomena occur beyond the regime of the Gaussian model we consider here. In the present study, to show that the deformed adsorption layer can generate the additional force exerted on the particle, we consider a simple preferential attraction; the additional free-energy density is assumed to be a linear function [11–16]. This does not contradict with the existence of the normal transition, as discussed at the end of Appendix A.

Our formulation is given in Sec. II. The following calculation is outlined and the result is shown in Sec. III. Our calculation is performed within the linear approximation of the fluctuation amplitude and on the assumption of weak preferential attraction. Equation (23) represents the small oscillation of the particle about the equilibrium point. From this equation, we can find the potential energy modified by the ambient near-criticality. Applying the equipartition theorem, we find the mean square displacement to be given by Eq. (25), instead of the first equation of Eq. (1). We cannot obtain this result by regarding the mixture as a simple bath, as shown in Appendix B. Our calculation procedure is described in Sec. IV, with some further details being relegated to Appendix C. The procedure becomes rather involved because a boundary layer appears in the limit of vanishing interdiffusion. We

discuss the result by using typical values of material constants and give some outlook in Sec. V.

## II. FORMULATION

For the mass-density difference between the two components, we write  $\varphi$ , which depends on the position  $\mathbf{r}$  in the mixture. As mentioned in Sec. I, we assume the  $\varphi$ -dependent part of the free-energy functional to be

$$\int_{C^e} d\mathbf{r} \left\{ f(\varphi(\mathbf{r})) + \frac{1}{2} M |\nabla \varphi(\mathbf{r})|^2 \right\} + \int_{\partial C} dS f_s(\varphi(\mathbf{r})) , \quad (5)$$

where the coefficient  $M$  is a positive constant. The first term is the volume integral over the mixture region ( $C^e$ ), while the second is the surface integral over the particle surface ( $\partial C$ ). We assume the Gaussian model and the preferential attraction caused by the surface field;  $f$  is a quadratic function and  $f_s$  is a linear function. We write  $h$  for the surface field, which is a constant defined as  $-f'_s = -df_s(\varphi)/(d\varphi)$ . Hereafter, the prime indicates the derivative with respect to the variable, and the double prime indicates the second derivative.

If we regard the mixture as a simple bath, we can calculate the mean square displacement directly from Eq. (5). Then, the chemical potential is homogeneous and constant, and the profile of  $\varphi$  is shifted translationally to follow the particle motion, *i.e.*, the adsorption layer of Fig. 1(a) moves as it is even when the particle moves. Details are shown in Appendix B. Thus, the total force exerted on the particle by the mixture always vanishes in this calculation, which should be incorrect because the chemical potential is changed locally by the particle motion in practice. To take this change into account, we use the reversible dynamics based on Eq. (5), as mentioned in Sec. I. We write  $\mathbf{v}$  for the velocity field in the mixture. Assuming the mass density of the mixture  $\rho$  to be a constant, we have

$$\nabla \cdot \mathbf{v}(\mathbf{r}, t) = 0 . \quad (6)$$

The chemical potential is given by

$$\mu(\mathbf{r}, t) = f'(\varphi(\mathbf{r}, t)) - M \Delta \varphi(\mathbf{r}, t) , \quad (7)$$

while the local equilibrium at the interface gives [6, 15]

$$M \mathbf{n} \cdot \nabla \varphi = -h \quad \text{at } \partial C . \quad (8)$$

Here,  $\mathbf{n}$  denotes the unit vector which is normal to the particle surface and is directed outwards. We need not assume the viscosity to calculate the equal-time correlation, and have

$$\rho \frac{\partial \mathbf{v}}{\partial t} = -\nabla p - \varphi \nabla \mu , \quad (9)$$

where the convective term is neglected in anticipation of the later linear approximation. The scalar  $p$  originates from the  $\rho$ -dependent part of the free energy, but can be regarded as dependent on  $\mathbf{r}$  and  $t$  irrespective of the local state in the incompressible fluid. The boundary-layer problem appears in the limit of the zero viscosity. We can deal with this problem by assuming the slip boundary condition at the particle surface. There, the tangential components of the velocity need not be continuous, while the normal component is continuous. The stress exerted on the particle is evaluated immediately outside the boundary layer.

The diffusive flux between the two components is proportional to the gradient of  $\mu$ . The mass conservation of each component leads to

$$\frac{\partial \varphi}{\partial t} = -\mathbf{v} \cdot \nabla \varphi + L \Delta \mu , \quad (10)$$

where the Onsager coefficient  $L$  is assumed to be a positive constant. The diffusion flux cannot pass across the particle surface, which leads to

$$\mathbf{n} \cdot L \nabla \mu = 0 \quad \text{at } \partial C . \quad (11)$$

The diffusion should not be involved in the reversible dynamics, and we should take the limit of  $L \rightarrow 0+$ . (Here,  $0+$  means that the limit  $L \rightarrow 0$  is taken with  $L > 0$  maintained.) However, care should be taken because  $L$  is associated with the highest-order derivative in Eq. (10) [24]. The limit  $L \rightarrow 0+$  causes another boundary-layer problem, which is unfamiliar unlike the problem in the limit of zero viscosity, if  $h$  does not vanish. Hence, we do not take the limit of  $L \rightarrow 0+$  until we get able to examine the influence of the boundary layer. Details are shown in Sec. IV D. A similar problem was encountered in Ref. 25, where the present author studied the ambient near-criticality of a fluid membrane fluctuating around a plane. Whether the surface is flat or curved is not significant to the thin boundary layer. The thickness of this boundary layer of the chemical potential vanishes in the limit of  $L \rightarrow 0+$  in the present study, as well as in the previous study.

Far from the particle, the mixture is assumed to be static and in the homogeneous phase, *i.e.*,  $\mathbf{v}$  vanishes and  $\varphi$  is constant. There,  $\mu$  and  $p$  are constants, considering Eqs. (7) and (9). We write  $\varphi_\infty$ ,  $\mu^{(0)} \equiv f'(\varphi_\infty)$ , and  $p^{(0)}$  for the constant values of  $\varphi$ ,  $\mu$ , and  $p$ , respectively. We assume the Gaussian model,

$$f(\varphi) = \frac{a}{2} (\varphi - \varphi_\infty)^2 + \mu^{(0)} (\varphi - \varphi_\infty) . \quad (12)$$

Here,  $a$  is a positive constant proportional to  $T - T_c$ , where  $T_c$  denotes the critical temperature. The correlation length far from the particle, denoted by  $\xi_c$ , is given by  $\sqrt{M/a}$ . We nondimensionalize it to define  $s_c$  as

$$s_c \equiv \frac{\xi_c}{r_0} = \frac{1}{r_0} \sqrt{\frac{M}{a}} , \quad (13)$$

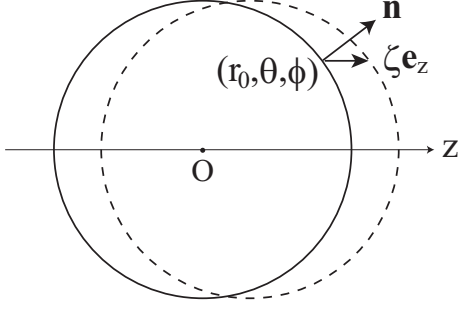


FIG. 2: We draw a cross section including the  $z$ -axis. The bottom of the harmonic potential is fixed at the origin  $O$ . In the unperturbed state, the particle center is fixed at  $O$  and the particle surface is represented by the solid circle. A point on the surface, with its spherical coordinate given by  $(r_0, \theta, \phi)$ , moves when the particle is shifted;  $r_0$  denotes the particle radius. A transient particle surface is drawn with the dashed circle, and the displacement vector of the point is given by  $\zeta \mathbf{e}_z$ . The unit normal vector  $\mathbf{n}$  at the point remains unchanged in the particle motion. The dimensionless radial length is defined as  $s \equiv r/r_0$ .

where  $r_0$  denotes the particle radius.

We take the spherical polar coordinates  $(r, \theta, \phi)$ , locating the origin at the bottom of the harmonic potential imposed externally. The particle motion is assumed to be along the  $z$ -axis (polar axis);  $\mathbf{e}_z$  denotes the unit vector in the  $z$ -direction (Fig. 2). We write  $\zeta(t)$  for the  $z$ -coordinate of the particle center. The total force exerted on the particle by the mixture is along the  $z$ -axis; its  $z$ -component is denoted by  $\mathcal{F}_z(t)$ . The reversible dynamics of the particle is given by

$$m \frac{d^2}{dt^2} \zeta(t) = \mathcal{F}_z(t) - m\omega_0^2 \zeta(t) \quad (14)$$

instead of Eq. (3). We should calculate  $\mathcal{F}_z$  from the fields of the mixture. Let us introduce a dimensionless parameter  $\varepsilon$  so that we have

$$\zeta(t) = \varepsilon \zeta^{(1)}(t). \quad (15)$$

Assuming  $|\varepsilon|$  to be small, we below calculate  $\mathcal{F}_z$  up to the order of  $\varepsilon$ .

The equilibrium state occurring when the particle center is fixed at the origin is regarded as the reference state, or the unperturbed state, where  $\mu$  is homogeneous over a mixture region and so is  $p$  because of Eq. (9) [15]. They are respectively given by the constants  $\mu^{(0)}$  and  $p^{(0)}$ . The superscript  $(0)$  is used to indicate the field in the unperturbed state. Because of the symmetry of the unperturbed state,  $\varphi^{(0)}$  depends only on  $r \equiv |\mathbf{r}|$ . As shown in Sec. IV B, we find it to be given by

$$\varphi^{(0)}(r) = \varphi_\infty + \frac{hr_0 e^{(1-s)/s_c}}{Ms(1+s_c^{-1})}, \quad (16)$$

where  $s \equiv r/r_0$  is the dimensionless radial length. This result is obtained in Ref. [8] and is used in Ref. [15]. Up to the order of  $\varepsilon$ , we expand the fields as

$$\begin{aligned} \varphi(\mathbf{r}, t) &= \varphi^{(0)}(r) + \varepsilon \varphi^{(1)}(\mathbf{r}, t), \\ \mu(\mathbf{r}, t) &= \mu^{(0)} + \varepsilon \mu^{(1)}(\mathbf{r}, t), \\ p(\mathbf{r}, t) &= p^{(0)} + \varepsilon p^{(1)}(\mathbf{r}, t), \\ \text{and } \mathbf{v}(\mathbf{r}, t) &= \varepsilon \mathbf{v}^{(1)}(\mathbf{r}, t). \end{aligned} \quad (17)$$

The field with the superscript  $(1)$  is defined so that it becomes proportional to  $\varepsilon$  after being multiplied by  $\varepsilon$ . The fields with the superscript  $(1)$  in Eq. (17) vanish far from the particle.

### III. RESULT

We add an overtilde to the Fourier transform with respect to  $t$ , e.g.,

$$\tilde{p}^{(1)}(\mathbf{r}, \omega) = \frac{1}{2\pi} \int_{-\infty}^{\infty} dt p^{(1)}(\mathbf{r}, t) e^{i\omega t}. \quad (18)$$

Let  $(r, \theta, \phi)$  be the components of the positional vector  $\mathbf{r}$  in the mixture. Using a spherical harmonics  $Y_{10}(\theta) = \sqrt{3/(4\pi)} \cos \theta$ , because of the symmetry of the state, we can assume

$$\tilde{p}^{(1)}(\mathbf{r}, \omega) = p_{10}(r, \omega) Y_{10}(\theta), \quad (19)$$

whereby the coefficient function  $p_{10}$  is defined. Similarly, we introduce the coefficient functions for the Fourier transforms of the other mixture fields at the order of  $\varepsilon$ . From Eqs. (6), (7), (9), and (10), we can obtain a set of simultaneous equations with respect to these coefficient functions. The equations are given by Eqs. (41), (44), and (56) in the next section. To solve them approximately, we assume the preferential attraction to be weak.

We define  $\Xi(s)$  so that  $\varphi^{(0)'}(r)$  equals  $r_0 \Xi(s) \varphi^{(0)''}(r_0)$ , i.e.,

$$\Xi(s) = -\frac{s + s_c}{s^2 \kappa (1 + s_c)} e^{(1-s)/s_c}, \quad (20)$$

where we use

$$\kappa \equiv 2s_c + \frac{1}{1 + s_c}. \quad (21)$$

We have  $\varphi^{(0)''}(r_0) = h\kappa/(Mr_0)$  because of Eq. (16). Let us define a positive dimensionless parameter  $\Lambda$  so that we have

$$\Lambda^2 \equiv \frac{h^2 \kappa}{\rho \omega^2 r_0^2 M}. \quad (22)$$

The calculation in Sec. IV E supposes  $\Lambda^2 \ll 1$ , which holds when  $h^2$  is sufficiently small, i.e., when the preferential attraction is sufficiently weak. This inequality

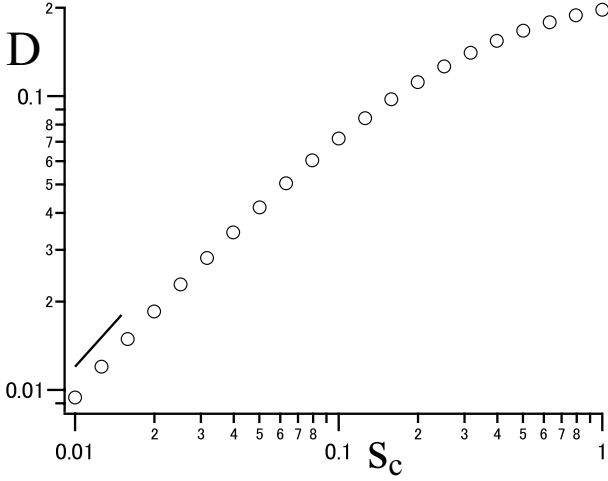


FIG. 3: Circles represent  $D(s_c)$  calculated from Eq. (24). The slope of the unity is shown by the short line for a reference.

condition is paraphrased more conveniently at the end of Sec. IV E.

After the calculation shown in Sec. IV, we can rewrite Eq.(14) as

$$\left(m + \frac{2\pi\rho r_0^3}{3}\right) \frac{d^2\zeta}{dt^2} = -[m\omega_0^2 \{1 + \lambda^2 D(s_c)\}] \zeta \quad (23)$$

up to the order of  $\varepsilon$ . This represents the small oscillation of the particle about the equilibrium point. Here,  $\lambda$  is a dimensionless parameter defined as  $h\sqrt{6\pi r_0/(Mm)}/\omega_0$ ;  $D$  is defined as

$$D(s_c) \equiv 2\kappa^2 \int_1^\infty ds \frac{\Xi(s)^2}{s^6}, \quad (24)$$

which is plotted in Fig. 3 with the aid of the software Mathematica (Wolfram Research). The second term in the parentheses on the left-hand side (lhs) of Eq. (23) represents the induced mass, which equals half the mass of the displaced mixture, as stated below Eq. (1). We can derive  $D(s_c) \approx s_c$  for small  $s_c$ , as shown by Eq. (C13). In agreement with this, the numerical results in Fig. 3 for small  $s_c$  have the slope of about the unity.

From Eq. (23), we apply the equipartition law to obtain

$$\langle \zeta^2 \rangle = k_B T \left\{ m\omega_0^2 + \frac{6\pi h^2 r_0}{M} D(s_c) \right\}^{-1}, \quad (25)$$

which gives the mean square displacement of the particle. The sum in the brackets of Eq. (25) is the same as the one in the braces of Eq. (23). Comparing Eq. (25) with the first equation of Eq. (1), we find the second term in the brackets of Eq. (25) to represent the effect of the ambient near-criticality, which reduces the mean square displacement, *i.e.* suppresses the fluctuation amplitude. The suppression effect is more marked as  $h^2$  is larger

and as  $\xi_c$  is larger. Then, the adsorption layer is also remarkable in its thickness and amplitude, considering Eq. (16).

## IV. CALCULATION PROCEDURE

We here describe the calculation procedure leading to Eq. (23).

### A. Pressure tensor

From the first term of Eq. (5), the reversible part of the pressure tensor is derived as [15, 17]

$$\Pi = \left(p - f + \mu\varphi - \frac{M}{2} |\nabla\varphi|^2\right) \mathbf{1} + M\nabla\varphi\nabla\varphi, \quad (26)$$

where  $\mathbf{1}$  denotes the isotropic tensor and  $\mu$  is given by Eq. (7). In the above,  $\varphi f' - f$  gives the osmotic pressure [26]. Because  $\nabla \cdot \Pi$  equals  $\nabla p + \varphi \nabla \mu$ , we have Eq. (9). Let the local stress exerted on the particle by the ambient mixture be denoted by  $\mathbf{F}(\mathbf{r}_s, t)$ , where  $\mathbf{r}_s$  represents a point on the particle surface. We have

$$\mathbf{F}(\mathbf{r}_s, t) = -\Pi \cdot \mathbf{n} + \nabla_{\parallel} f_s - \frac{2f_s}{r_0} \mathbf{n}. \quad (27)$$

Here,  $\nabla_{\parallel}$  implies the projection of  $\nabla$  on the tangent plane and  $1/r_0$  gives the mean curvature of the particle surface. The last two terms above come from the stress due to the two-dimensional pressure  $-f_s$ , as discussed in Appendix A of Ref. 13. The tangential components of  $\mathbf{F}$  vanishes; the contribution from  $M\nabla\varphi\nabla\varphi$  of Eq. (26) cancels with the tangential stress due to  $f_s$ , as described in Appendix D of Ref. 13. In fact, we use Eq. (8) to rewrite the right-hand side (rhs) of Eq. (27) as

$$\left(-p + f + \frac{M}{2} |\nabla\varphi|^2 - \mu\varphi - \frac{h^2}{M} - \frac{2f_s}{r_0}\right) \mathbf{n}, \quad (28)$$

which is evaluated immediately outside the boundary layer generated in the limit of zero viscosity. See the statement below Eq. (9).

### B. Profile in the unperturbed state

We write  $\partial_r$  for the differentiation with respect to  $r$ , and  $\partial_r^2$  for  $\partial_r \partial_r$ . As argued for a mixture in contact with a flat wall [6], Eq. (7) yields

$$f'(\varphi^{(0)}) - \frac{M}{r} \partial_r^2 r \varphi^{(0)} = \mu^{(0)}, \quad (29)$$

while Eq. (8) yields

$$M \frac{\partial}{\partial r} \varphi^{(0)} = -h \quad \text{as } r \rightarrow r_0 +. \quad (30)$$

Solving these equations, we arrive at Eq. (16). The equilibrium profile of the concentration difference around a sphere was studied on conditions other than considered here [27–30].

### C. Equations at the order of $\varepsilon$

Suppose a point,  $(r_0, \theta, \phi)$ , on the particle surface in the unperturbed state (Fig. 2). By the particle motion, its  $z$ -coordinate changes from  $z_0 \equiv r_0 \cos \theta$  to  $z_0 + \zeta$ . The slip boundary condition up to the order of  $\varepsilon$  gives

$$v_r^{(1)} \Big|_{z_0} = \frac{\partial \zeta^{(1)}}{\partial t} \cos \theta , \quad (31)$$

where the subscript  $z_0$  means that the term is evaluated at the point on surface in the unperturbed state,  $(r_0, \theta, \phi)$ . Equation (8) is rewritten as

$$-h = M \mathbf{n} \cdot \nabla \varphi \Big|_{z_0 + \zeta} , \quad (32)$$

where the subscript  $z_0 + \zeta$  means that the term is evaluated at the point on surface of the shifted particle. The unit normal vector  $\mathbf{n}$  remains the same during the particle motion (Fig. 2). We have

$$\varphi \Big|_{z_0 + \zeta} = \varphi^{(0)} \Big|_{z_0 + \zeta} + \varepsilon \varphi^{(1)} \Big|_{z_0} + \mathcal{O}(\varepsilon^2) , \quad (33)$$

where  $\mathcal{O}(\varepsilon^2)$  means the terms whose quotient divided by  $\varepsilon^2$  remain finite in the limit of  $\varepsilon \rightarrow 0$ . The first term on the rhs above is rewritten as

$$\varphi^{(0)}(r_0) + \zeta \frac{\partial}{\partial z} \varphi^{(0)}(r) \Big|_{z_0} . \quad (34)$$

Considering Eq. (30), we use these three equations to obtain

$$\frac{\partial}{\partial r} \varphi^{(1)} \Big|_{z_0} = -\zeta^{(1)} \varphi^{(0)''}(r_0) \cos \theta . \quad (35)$$

Using Eqs. (29), (30), and (35), we rewrite Eq. (28) so that it is evaluated on the particle surface in the unperturbed state. Integrating the result over the surface, we obtain up to the order of  $\varepsilon$

$$\begin{aligned} \mathcal{F}_z = 2\varepsilon\pi r_0^2 \int_0^\pi d\theta \sin \theta \cos \theta \left[ -p^{(1)} - \mu^{(1)} \varphi^{(0)} \right. \\ \left. + \left( \varphi^{(1)} - \frac{h}{M} \zeta^{(1)} \cos \theta \right) \left\{ \frac{2h}{r_0} + \frac{M}{r_0} \partial_r^2 r \varphi^{(0)} \right\} \right] \end{aligned} \quad (36)$$

where the integrand is evaluated at  $(r_0, \theta, \phi)$ . We define  $\mathcal{F}_z^{(1)}$  so that  $\mathcal{F}_z$  equals  $\varepsilon \mathcal{F}_z^{(1)}$  up to the order of  $\varepsilon$ .

As in Eq. (19), we define coefficient functions  $Q_{10}$  and  $G_{10}$  so that we have

$$\begin{aligned} \tilde{\mu}^{(1)}(\mathbf{r}, \omega) &= Q_{10}(r, \omega) Y_{10}(\theta) \\ \text{and } \tilde{\varphi}^{(1)}(\mathbf{r}, \omega) &= G_{10}(r, \omega) Y_{10}(\theta) . \end{aligned} \quad (37)$$

We use the vector spherical harmonics,

$$\mathbf{P}_{10}(\theta, \phi) = \mathbf{e}_r Y_{10} \text{ and} \quad (38)$$

$$\mathbf{B}_{10}(\theta, \phi) = \frac{1}{\sqrt{2}} \mathbf{e}_\theta \frac{\partial}{\partial \theta} Y_{10}(\theta) , \quad (39)$$

where  $\mathbf{e}_r$  and  $\mathbf{e}_\theta$  denote the unit vectors tangent to the coordinate line of  $r$  and curve  $\theta$ , respectively. As in Ref. 15, we can assume

$$\tilde{\mathbf{v}}^{(1)}(\mathbf{r}, \omega) = R_{10}(r, \omega) \mathbf{P}_{10}(\theta, \phi) + T_{10}(r, \omega) \mathbf{B}_{10}(\theta, \phi) , \quad (40)$$

where functions  $R_{10}$  and  $T_{10}$  are introduced.

Using Eqs. (19) and (40) in Eqs. (6) and (9), we obtain Eqs. (C1), (C2), and (C3), which generate

$$\frac{r^2}{2} \partial_r^2 R_{10} + 2r \partial_r R_{10} = \frac{\varphi^{(0)'} Q_{10}}{i\rho\omega} . \quad (41)$$

We introduce  $\zeta_{10}$  so that we have

$$\tilde{\zeta}^{(1)}(\omega) = \sqrt{\frac{3}{4\pi}} \zeta_{10}(\omega) . \quad (42)$$

Equation (31) yields

$$R_{10} \Big|_{z_0} = -i\omega \zeta_{10} , \quad (43)$$

and  $R_{10}$  vanishes far from the particle, as stated below Eq. (17). If  $h$  vanishes,  $\mu$  and  $\varphi$  are constant; the constant solutions satisfy Eqs. (7), (8), (10), and (11) together with the boundary conditions far from the particle. Then, we find  $R_{10}(r, \omega) = -i\omega \zeta_{10} r_0^3 / r^3$  from Eq. (41) and the boundary conditions. Thus, otherwise,  $R_{10}$  is given by the sum of this solution for  $h = 0$  and terms dependent on  $h$ .

Equation (10) yields

$$-i\omega G_{10} = -R_{10} \varphi^{(0)'} + L \left( \partial_r^2 + \frac{2}{r} \partial_r - \frac{2}{r^2} \right) Q_{10} . \quad (44)$$

If we assume  $L$  to vanish from the beginning, Eq. (44) gives

$$i\omega G_{10} = R_{10} \varphi^{(0)'} , \quad (45)$$

which is differentiated with respect to  $r$  to give  $\varphi^{(0)'} \partial_r R_{10} = 0$  at  $r \rightarrow r_0 +$  with the aid of Eq. (35). Thus, then, we have  $\partial_r R_{10} \rightarrow 0$  at  $r \rightarrow r_0 +$  for  $h \neq 0$ . It is impossible to impose this boundary condition for any nonzero  $h$  because Eq. (41) has other two boundary conditions mentioned at and below Eq. (43). This contradiction means that, if  $h$  does not vanish, Eq. (45) is valid only outside the boundary layer. Then, even when  $L$  approaches zero, the second term on the rhs of Eq. (44) cannot be neglected inside the boundary layer because of steep change of  $Q_{10}$ . The solution outside the boundary layer is called outer solution [24]. Equation (45) thus holds only if  $G_{10}$  and  $R_{10}$  are replaced by their respective outer solutions.

### D. Nondimensionalization

We introduce dimensionless fields

$$\mathcal{G}(s, \omega) \equiv \frac{MG_{10}(r, \omega)}{h\kappa\zeta_{10}(\omega)}$$

$$\text{and } \mathcal{Q}(s, \omega) \equiv \frac{r_0^2 Q_{10}(r, \omega)}{h\zeta_{10}(\omega)}, \quad (46)$$

which do not diverge when  $h$  vanishes because of the statement below Eq. (43). Hereafter, we sometimes write  $\mathcal{G}$  or  $\mathcal{G}(s)$  for  $\mathcal{G}(s, \omega)$ , and write  $\mathcal{G}'$  for  $\partial_s \mathcal{G}$ . These ways of writing are also applied for  $\mathcal{Q}$  and  $\mathcal{R}$ . From Eq. (35) and the statement below Eq. (17), we have

$$\mathcal{G}' \rightarrow -s_c^{-1} \text{ as } s \rightarrow 1+ \text{ and } \mathcal{G} \rightarrow 0 \text{ as } s \rightarrow \infty. \quad (47)$$

From Eq. (11) and the statement below Eq. (17), we have

$$\mathcal{Q}' \rightarrow 0 \text{ as } s \rightarrow 1+ \text{ and } \mathcal{Q} \rightarrow 0 \text{ as } s \rightarrow \infty. \quad (48)$$

We write  $\mathcal{G}_{\text{out}}$  and  $\mathcal{R}_{\text{out}}$  for the outer solutions of  $\mathcal{G}$  and  $\mathcal{R}$ , respectively. Equation (45) gives

$$\mathcal{G}_{\text{out}} = -\Xi \mathcal{R}_{\text{out}}. \quad (49)$$

Introducing

$$\mathcal{R}(s, \omega) \equiv \frac{iR_{10}(r, \omega)}{\omega\zeta_{10}(\omega)}, \quad (50)$$

we rewrite Eq. (41) as

$$\left( \frac{s^2}{2} \partial_s^2 + 2s \partial_s \right) \mathcal{R} = \Lambda^2 \Xi \mathcal{Q}. \quad (51)$$

Equation (43) and the statement below it give

$$\mathcal{R} \rightarrow 1 \text{ as } s \rightarrow 1+ \text{ and } \mathcal{R} \rightarrow 0 \text{ as } s \rightarrow \infty. \quad (52)$$

Applying the method of variation of parameters to Eqs. (51) and (52), we obtain

$$\mathcal{R}(s) = s^{-3} + \frac{2}{3} \Lambda^2 \int_1^\infty d\sigma \Gamma_R(s, \sigma) \Xi(\sigma) \mathcal{Q}(\sigma), \quad (53)$$

where the kernel is defined by

$$\Gamma_R(s, \sigma) = \begin{cases} s^{-3} \sigma^{-1} (1 - \sigma^3) & \text{for } \sigma < s \\ s^{-3} \sigma^{-1} (1 - s^3) & \text{for } s \leq \sigma \end{cases}. \quad (54)$$

Picking up terms at the order of  $\varepsilon$  of Eq. (7) yields

$$-\mu^{(1)} = (M\Delta - a) \varphi^{(1)}. \quad (55)$$

Substituting Eq. (37) into the Fourier transform of Eq. (55), we obtain

$$-\mathcal{Q} = \kappa \left( \partial_s^2 + \frac{2}{s} \partial_s - \frac{2}{s^2} - \frac{1}{s_c^2} \right) \mathcal{G} \quad (56)$$

with the aid of Eq. (46). Applying the method of variation of parameters to Eq. (56), we use the second condition of Eq. (47) to obtain

$$\mathcal{G}(s) = s_c \mathcal{G}'(1+) \Xi(s) + \frac{s_c}{\kappa \sqrt{s}} \int_1^\infty d\sigma \sqrt{\sigma} \Gamma_G(s, \sigma) \mathcal{Q}(\sigma), \quad (57)$$

where the kernel  $\Gamma_G$  is defined by Eq. (C6) and  $\mathcal{G}'(1+)$  denotes  $\mathcal{G}'(s)$  at  $s \rightarrow 1+$ . Because of the first condition of Eq. (47), we can substitute  $-s_c^{-1}$  into  $\mathcal{G}'(1+)$  above.

We can define  $\mathcal{Q}_{\text{out}}(s, \omega)$  for  $s > 1$  in the limit of  $L \rightarrow 0+$ . Subtracting it from  $\mathcal{Q}(s, \omega)$ , we define  $\mathcal{Q}_{\text{in}}(s, \omega)$  as the difference. It vanishes outside the boundary layer, but cannot be neglected in the following integral. Assuming that  $s$  lies outside the boundary layer in Eq. (57), we obtain

$$\mathcal{G}_{\text{out}}(s) = -\Xi(s) \left\{ 1 + \frac{s_c}{\kappa} \int_0^\infty d\sigma \mathcal{Q}_{\text{in}}(\sigma) \right\} + \frac{s_c}{\kappa \sqrt{s}} \int_1^\infty d\sigma \sqrt{\sigma} \Gamma_G(s, \sigma) \mathcal{Q}_{\text{out}}(\sigma) \quad (58)$$

in the limit of  $L \rightarrow 0+$ .

### E. Weak preferential attraction

Assuming  $\Lambda^2 \ll 1$ , we below obtain  $\mathcal{Q}$  up to the order of  $\Lambda$  and use the result in Eq. (53) to calculate  $\mathcal{R}$  up to the order of  $\Lambda^3$ . To begin with, from Eqs. (49) and (53), we derive

$$\mathcal{G}_{\text{out}}(s) = -\frac{\Xi(s)}{s^3} + \mathcal{O}(\Lambda^2), \quad (59)$$

which leads to

$$\mathcal{G}'_{\text{out}}(1+) = -\frac{1}{s_c} - \frac{3}{\kappa} + \mathcal{O}(\Lambda^2). \quad (60)$$

Equation (56) remains valid if  $\mathcal{Q}$  and  $\mathcal{G}$  are respectively replaced by  $\mathcal{Q}_{\text{out}}$  and  $\mathcal{G}_{\text{out}}$ . Thus, we can do the same replacement in Eq. (57) although  $\mathcal{G}'_{\text{out}}(1+)$  is given not by the first condition of Eq. (47) but by Eq. (60). Thus, in the limit of  $L \rightarrow 0+$ , we find [31]

$$\begin{aligned} & \frac{s_c}{\kappa \sqrt{s}} \int_1^\infty d\sigma \sqrt{\sigma} \Gamma_G(s, \sigma) \mathcal{Q}_{\text{out}}(\sigma) \\ &= -s^{-3} \Xi(s) + \left( 1 + \frac{3s_c}{\kappa} \right) \Xi(s) + \mathcal{O}(\Lambda^2). \end{aligned} \quad (61)$$

Substituting Eq. (61) into Eq. (58), we use Eq. (59) to obtain

$$\int_0^\infty d\sigma \mathcal{Q}_{\text{in}}(\sigma) = 3 + \mathcal{O}(\Lambda^2) \quad (62)$$

Taking the limit of  $s \rightarrow 1+$  in Eq. (57), we use Eqs. (61) and (62) to find

$$\mathcal{G}(1+) = \frac{1}{\kappa} + \mathcal{O}(\Lambda^2) \quad (63)$$

with the aid of Eqs. (20) and (21). Thus, up to the order of  $\Lambda$ , the difference in the parentheses of Eq. (36) vanishes. We can rewrite the first two terms in the brackets of Eq. (36) by using Eqs. (C1) and (C3). Using this result and Eq. (52), we obtain

$$\tilde{\mathcal{F}}_z^{(1)}(\omega) = -\frac{2\pi\rho\omega^2 r_0^3}{3} \{2 + \mathcal{R}'(1+) + \mathcal{O}(\Lambda^4)\} \zeta^{(1)}. \quad (64)$$

As shown in Appendix C, we can utilize Eqs. (53) and (62) to obtain

$$\mathcal{R}'(1+) = -3 + 18\Lambda^2\kappa \int_1^\infty ds \frac{\Xi(s)^2}{s^6} + \mathcal{O}(\Lambda^4). \quad (65)$$

From Eqs. (14), (64), and (65), we can derive Eq. (23). In its brackets, terms of  $\mathcal{O}(\lambda^4)$  are neglected.

It is usual that the specific gravity of the particle is around the unity. The Fourier transform of Eq. (23) determines the normal-mode frequency  $\omega$ , which deviates from  $\omega_0$  mainly because of the induced mass in our calculation done on the assumption of weak preferential attraction. Thus, the frequency is about  $\sqrt{2/3}\omega_0$ , which can replace  $\omega$  in evaluating Eq. (22). As mentioned in the fourth paragraph of Sec. I,  $s_c = \xi_c/r_0 \ll 1$  is assumed in our hydrodynamics, which leads to  $\kappa \approx 1$  in Eq. (21). Thus, the condition  $\Lambda^2 \ll 1$  can be identified with  $\lambda^2/3 \ll 1$ . Judging from the definition of  $\lambda$  given above Eq. (24), we find that our approximate calculation supposes  $\omega_0 \neq 0$ . It is reasonable, considering that the deformation of the adsorption layer becomes smaller as the particle moves more slowly.

## V. DISCUSSION

The present author recently studied the mean square amplitude of the shape fluctuation of a fluid membrane immersed in a near-critical binary fluid mixture in the same framework as used in the present study, and showed that the ambient near-criticality tends to suppress the membrane undulation [25]. Although the particle considered here is not deformed during its motion, unlike the membrane, the suppression effect in our present result is well expected from the previous result. We can calculate  $\varphi^{(1)}$  approximately from the first term on the rhs of Eq. (59). Comparing the values of  $\varphi$  at the two points on the  $z$ -axis immediately outside the particle, we find that, if  $h$  is positive, the value at  $z = r_0 + \zeta$  is larger (smaller) than the value at  $z = -r_0 + \zeta$  when  $\zeta$  is positive (negative). Thus, within the approximation, the local difference of the mass density of the disliked component subtracted from the mass density of the preferred component is larger on the front side of the moving particle than that of the rear side. This situation is shown by Fig. 1(b) if we regard the gray scale as representing the deviation

of the local difference from its value far from the particle.

For example, suppose a mixture of nitroethane and 3-methylpentane, which has  $T_c = 300$  K. The mixture has  $\xi_c \approx 10$  nm for  $T - T_c \approx 0.3$  K at the critical fraction [32]. On the basis of the discussion in Ref. 29,  $h \approx 10^{-6}$  m<sup>3</sup>/s<sup>2</sup> is estimated in Ref. 25 for a glass surface and an organic mixture, between which the hydrogen bonding is made significantly. This value would be overestimated for such a surface as cannot make hydrogen bonding so much. We use  $h = 10^{-7}$  m<sup>3</sup>/s<sup>2</sup>. The coefficient of the square gradient term in the free-energy density is sometimes called influence parameter [33, 34]. The parameter can be defined in general for each pair of the components,  $A$ - $A$ ,  $B$ - $B$ , and  $A$ - $B$ , where  $A$  and  $B$  represent the kinds of the two components. The coefficient  $M$  is for the last pair, which can be regarded roughly as the geometric mean of the parameters for the first two pairs [35]. We cannot find out the data for the influence parameters of the mixture mentioned above. Judging from the data for the pure fluid of alkane, we use  $M = 10^{-16}$  m<sup>7</sup>/(s<sup>2</sup>kg) [36]. For these parameter values, as discussed below Eq. (A7), longer correlation length than about 10 nm cannot be assumed in the regime of the Gaussian model.

The spring constant of the optical tweezers typically ranges from  $10^{-3}$  to  $10^{-6}$  kg/s<sup>2</sup> [37]. Let us assume it to be  $m\omega_0^2 = 4.14 \times 10^{-4}$  kg/s<sup>2</sup>, which leads to  $\langle \zeta^2 \rangle \approx 10$  nm<sup>2</sup> in Eq. (1) without the ambient near-criticality being assumed. Suppose a particle having  $r_0 = 100$  nm with the specific gravity being about the unity. We have  $s_c = 0.1$  for the value of  $\xi_c$  mentioned above. As mentioned in the fourth paragraph of Sec. I and at the end of Sec. IVE, our formulation supposes  $\xi_c \ll r_0$ , *i.e.*,  $s_c \ll 1$ , which is satisfied by the value above. The prefactor of  $D$  in Eq. (25) is calculated as  $6\pi h^2 r_0 / M \approx 2 \times 10^{-4}$  kg/s<sup>2</sup>. Thus, we have  $\lambda^2 \approx 0.48$ , which value satisfies the condition for the weak preferential attraction, mentioned at the end of Sec. IVE. According to Eq. (25),  $\langle \zeta^2 \rangle$  is reduced to about 9.5 nm<sup>2</sup> by the ambient near-criticality. Its square root is much smaller than  $r_0$ , which justifies the assumption of small amplitude of the particle fluctuation. The change of  $\langle \zeta^2 \rangle$  from 10 nm<sup>2</sup> to 9.5 nm<sup>2</sup> can be expected to be measured by means of the recent experimental technique, mentioned in Sec. I, although the increased turbidity in the near-critical mixture may make the measurement more delicate.

It is assumed in our calculation leading to the result, Eq. (25), that a rigid sphere fluctuates with small amplitude, that the mixture in the homogeneous phase is not very close to the critical point, and that the particle surface attracts one component weakly. Thus, we cannot apply the result beyond the parameter range generating weak suppression effect. Larger suppression effect may be observed experimentally in a setup with some ap-



appropriate parameter values. To predict this waits future theoretical studies not requiring the assumptions above. We also assume the preferential attraction to be caused by a short-ranged interaction and to be represented only by the surface field. How the suppression effect is altered without these assumptions also remains to be studied. We assume a particle size much larger than the correlation length to use the hydrodynamics based on the coarse-grained free-energy functional. For a smaller particle, the critical concentration fluctuation of the mixture would influence the particle motion, and a procedure other than used in the present study should be taken to calculate the mean square displacement. It is also a future problem.

### Acknowledgments

The author thanks K. Fukushima for the information of Ref. 40. Discussion with D. Goto is appreciated.

### Appendix A: Validity of the Gaussian model

Even beyond the regime of the Gaussian model, we can use the renormalized local functional theory, which is proposed by Okamoto and Onuki [38, 39]. They study the universal properties of a near-critical binary fluid mixture between two parallel walls or two spheres. We here assume that the mixture has the critical fraction far from the solid surface. The order parameter and the correlation length are not homogeneous, and are respectively denoted by  $\psi(\mathbf{r}) \equiv \varphi(\mathbf{r}) - \varphi_\infty$  and  $\xi(\mathbf{r})$ . The correlation length far from the surface, denoted by  $\xi_\infty$ , is asymptotically equal to  $\xi_0 \tau^{-\nu}$  as  $\tau$  approaches zero, where  $\xi_0$  is a nonuniversal constant,  $\tau \equiv (T - T_c)/T_c$  is assumed to be positive, and the critical exponent  $\nu$  is about 0.627 for the binary fluid mixture. In the Gaussian model,  $\xi_c$  is regarded as  $\xi_\infty$ . Below, we also use critical exponents  $\gamma \approx 1.239$  and  $\eta \approx 0.024$ .

In the Gaussian model, subtracting the volume integral of  $\mu^{(0)}\varphi$  from Eq. (5) with Eq. (12) gives the free-energy functional for the open system. Apart from an additional constant, the corresponding functional in the renormalized local functional theory can be obtained by replacing  $M$  and  $f - \mu^{(0)}\varphi$  respectively by  $C$  and  $f_R$  defined below. The coefficient  $C$  depends on  $\psi$  as

$$C(\psi) \equiv k_B T_c C_1 w^{-\eta\nu}, \quad (\text{A1})$$

where  $C_1$  is a nonuniversal constant and  $w$  is defined by  $w \equiv \xi_0^{1/\nu} \xi^{-1/\nu}$ , while  $f_R$  is given by

$$f_R(\psi) \equiv k_B T_c \left\{ \frac{1}{2} C_1 \xi_0^{-2} w^{\gamma-1} \tau \psi^2 + \frac{1}{4} C_1^2 u^* \xi_0^{-\epsilon} w^{\gamma-2\beta} \psi^4 \right\}, \quad (\text{A2})$$

as a result of the  $\epsilon$ -expansion. In later numerical calculations, we use  $\epsilon = 1$  and approximate the constant  $u^*$  to be  $2\pi^2/9$ . Equation (A2) is found to be the same as Eq. (3.5) of Ref. 38 with the aid of the scaling law  $(\epsilon - 2\eta)\nu = \gamma - 2\beta$ . Here, because the critical fraction is assumed far from the surface,  $\mu_\infty$  in Ref. 38 vanishes.

The free-energy functional after the replacement above is the one renormalized up to the local correlation length without rescaling, as in the exact renormalization group theory [40]. Thus, we can apply the mean-field theory to calculate  $\xi$  at each locus, which leads to

$$w = \tau + C_2 w^{1-2\beta} \psi^2, \quad (\text{A3})$$

where we use  $C_2 \equiv 3u^* C_1 \xi_0^{2-\epsilon}$ . These equations can be found in Ref. 38; see its Eqs. (3.9) and (3.11) and the statement below its Eq. (3.16). Defining  $U \equiv w/\tau$  and

$$s \equiv C_2 U^{1-2\beta} \tau^{-2\beta} \psi^2, \quad (\text{A4})$$

we rewrite Eq. (A3) as  $U = 1 + s$ . Equation (A2) is rewritten as

$$f_R(\psi) = \frac{k_B T_c C_1 \tau^{2\beta+\gamma}}{2C_2 \xi_0^2} U^{2\beta+\gamma-2} \left( s + \frac{s^2}{6} \right). \quad (\text{A5})$$

When  $s$  is much smaller than the unity over the mixture, the rhs of Eq. (A5) becomes  $C(\psi)\psi^2/(2\xi_\infty^2)$  approximately. Then, regarding  $C$  and  $\xi_\infty$  as  $M$  and  $\xi_c$ , respectively, we find that the Gaussian model is valid.

By using the free-energy functional introduced above, let us consider how large  $\xi_c$  we can assume in the Gaussian model for our problem. Limiting our discussion to cases of  $\xi_c \ll r_0$ , we assume the mixture to occupy the semi-infinite space bounded by a flat surface to estimate the upper limit of  $\xi_c$ . We here take the  $z$ -axis so that the mixture lies in  $z > 0$ . The order parameter is not rescaled in the renormalized local functional theory, and thus  $f_s$  remains unchanged in the renormalization process. As discussed in Sec. II B of Ref. 38, the order-parameter profile at the equilibrium is obtained by minimizing the free-energy functional because it is renormalized up to the local correlation length. Writing  $\bar{\psi}(z)$  for the profile, we obtain

$$C(\bar{\psi}(z)) \left| \frac{d\bar{\psi}(z)}{dz} \right|^2 = 2f_R(\bar{\psi}(z)) \quad (\text{A6})$$

for  $z > 0$ , and

$$C(\bar{\psi}(z)) \frac{d\bar{\psi}(z)}{dz} = -h \quad (\text{A7})$$

as  $z \rightarrow 0+$ . In the limit of  $z \rightarrow \infty$ ,  $\bar{\psi}(z)$  vanishes. We can derive the differential equation with respect to  $s(z)$  from Eqs. (A4), (A5), and (A6), while the algebraic equation with respect to  $s(0+)$  from Eqs. (A5), (A6), and (A7). The former shows that  $s(z)$  decreases

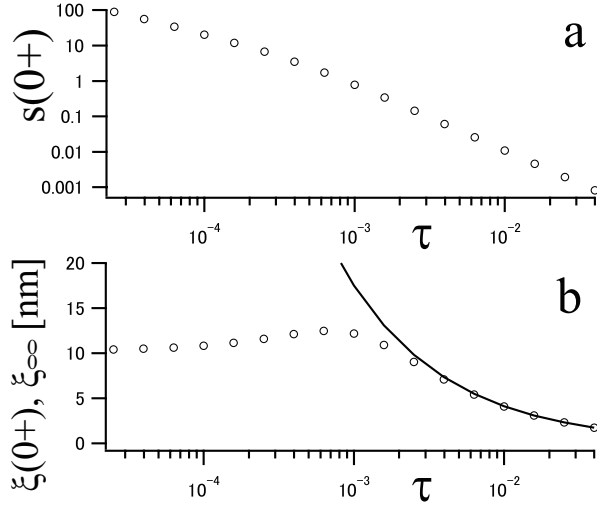


FIG. 4: (a) We calculate  $s(0+)$ , *i.e.*,  $\lim_{z \rightarrow 0+} s(z)$ , from Eqs. (A4) and (A7). (b) Circles represent  $\xi(0+)$ , while the solid curve represents  $\xi_\infty$ .

monotonically to zero as  $z$  increases from zero to infinity if  $h$  is positive [41]. Using the material constants mentioned in Sec. V, we numerically solve the latter to obtain Fig. 4(a). We find that  $s(0+)$  is much smaller than the unity when  $\tau$  is larger than about  $2 \times 10^{-3}$ . Then, we have  $s(z) \ll 1$  for any  $z > 0$  and the Gaussian model is valid. Calculating the correlation length immediately near the surface  $\xi(0+)$  from  $s(0+)$ , we plot the results in Fig. 4(b), where  $\xi_\infty$  is also plotted for comparison. They turn out to agree only when the Gaussian model is valid, and then  $\xi_\infty$  (or  $\xi_c$ ) is smaller than about 10 nm. As  $\tau$  is smaller,  $\xi(0+)$  reaches a plateau. This is because the preferential attraction prevents the mixture from approaching the critical point.

Below, we briefly show that the well-known universal profile near the flat surface can also be derived in the renormalized local functional theory. Details can be found in Ref. 41. When  $\tau$  decreases beyond the regime of the Gaussian model,  $s(0+)$  is much larger than the unity. Then, we have  $s(z) \gg 1$  up to a positive value of  $z$ . In this spacial region, Eqs. (A4), (A5), and (A6) lead to  $\bar{\psi}' \approx (s\tau)^{\beta+\nu} / (\sqrt{6C_2}\xi_0)$  when  $h$  is positive. Noting  $(s\tau)^\beta \approx \sqrt{C_2}\bar{\psi}$ , we find

$$\bar{\psi}(z) \approx \frac{1}{\sqrt{C_2}} \left\{ \frac{\sqrt{6}\beta\xi_0}{\nu(z+l_0)} \right\}^{\beta/\nu}, \quad (\text{A8})$$

where  $l_0$  is approximately equal to  $\sqrt{6}\beta\xi(0+)/\nu$ . We find that  $s(z) \gg 1$  is valid for  $z \ll \xi_\infty$ . For  $z \gg \xi_\infty$ , the profile is shown to exhibit the same exponential decay as shown in the Gaussian model. This is well known, as well as the profile of Eq. (A8) [42–44]. When  $\tau$  is sufficiently small, we have the region of  $l_0 \ll z \ll \xi_\infty$ ,

where Eq. (A8) can be regarded as

$$\bar{\psi}(z) \propto \left( \frac{\xi_0}{z} \right)^{\beta/\nu} = \tau^\beta \left( \frac{z}{\xi_\infty} \right)^{-\beta/\nu}, \quad (\text{A9})$$

which is consistent with the universal form [23, 43–45]. The profile of Eq. (A8) is the same as Eq. (2.15) of Ref. 38 for the case of  $\tau = 0$  and  $\bar{\psi}(\infty) = 0$  because of the statement below its Eq. (3.15). In this case, the region of the exponential decay vanishes, and the critical adsorption occurs.

Assuming  $f_s(\varphi)$  to be a linear function with a finite surface field, we can derive the universal form of the order-parameter profile, Eq. (A9). However,  $f_s(\varphi)$  can be a quadratic function. The negative of the coefficient of the second-order term is called surface enhancement. Neglecting the surface enhancement in the renormalized local functional theory, as is done above, should amount to assuming its bare value to be positive in the conventional renormalization group theory, where the surface enhancement is measured from the value at the special transition occurring at  $h = 0$ . See Ref. 23 and Eq. (3.95) of Ref. 21. We think that nonzero surface enhancement should not change remarkably the result in the present study, where the preferential attraction is assumed to be sufficiently weak.

## Appendix B: Naive average based on Eq. (5)

We here calculate the mean square displacement by regarding the mixture as a heat and particle bath. This procedure is incorrect, but is shown for comparison with the procedure described in the text. We define  $\Omega_b$  as the first term of Eq. (5) with  $f$  replaced by  $f - \mu^{(0)}\varphi$ , and define  $\Omega_s$  as the second term. We write  $\Omega$  for their sum. Suppose that  $\varphi$  and  $\zeta$  deviate from  $\varphi^{(0)}$  and zero, respectively. The resultant deviations of  $\Omega_b$ ,  $\Omega_s$ , and  $\Omega$ , denoted by  $\delta\Omega_b$ ,  $\delta\Omega_s$ , and  $\delta\Omega$ , respectively, are below calculated up to the second order with respect to  $\varphi_1 \equiv \varphi - \varphi^{(0)}$  and  $\zeta$ , as in Appendix of Ref. 25. We add the subscript  $\zeta$  to  $C^e$  and  $\partial C$  to indicate their dependence on  $\zeta$ . We find  $\delta\Omega_s[\varphi_1, \zeta]$  to be given by

$$\begin{aligned} & \int_{\partial C_\zeta} dS f_s(\varphi) - \int_{\partial C_0} dS f_s(\varphi^{(0)}) \\ &= -\frac{h\zeta^2}{2} \int_{\partial C_0} dS \frac{\partial^2}{\partial z^2} \varphi^{(0)} - h \int_{\partial C_\zeta} dS \varphi_1 \quad (\text{B1}) \end{aligned}$$

with the aid of Eq. (30). Similarly, writing  $\Phi^{(0)}$  for  $\varphi^{(0)} - \varphi_\infty$ , we find  $\delta\Omega_b[\varphi_1, \zeta]$  to be given by

$$\begin{aligned} & \int_{C_\zeta^e} d\mathbf{r} \left\{ a\Phi^{(0)} + M\nabla\varphi^{(0)} \cdot \nabla \right\} \varphi_1 \\ & - \frac{\zeta^2}{4} \int_{\partial C_0} dS \cos\theta \frac{\partial}{\partial z} \left\{ a\Phi^{(0)2} + M \left| \nabla\varphi^{(0)} \right|^2 \right\} \\ & + \frac{1}{2} \int_{C_0^e} d\mathbf{r} \left( a\varphi_1^2 + M |\nabla\varphi_1|^2 \right), \end{aligned} \quad (\text{B2})$$

which can be rewritten with the aid of Eqs. (29) and (30). The sum of Eqs. (B1) and (B2) gives  $\delta\Omega[\varphi_1, \zeta]$ , which is rewritten as

$$\begin{aligned} & \frac{1}{2} \int_{\partial C_0} dS \left\{ \zeta^2 h\varphi^{(0)''} \cos^2\theta - 2\zeta M\varphi^{(0)''} \varphi_1 \cos\theta \right. \\ & \left. - M\mathbf{n} \cdot (\varphi_1 \nabla\varphi_1) \right\} + \frac{1}{2} \int_{C_0^e} d\mathbf{r} (a\varphi_1^2 - M\Delta\varphi_1) \end{aligned} \quad (\text{B3})$$

with the aid of Eq. (30). Here, we also note that the surface integral of  $(1 - 3\cos^2\theta)$  over  $\partial C_0$  vanishes.

In this procedure, the probability density of  $\varphi_1$  and  $\zeta$  at the equilibrium is proportional to the Boltzmann weight,  $\exp(-\delta\Omega^+/k_B T)$ , where  $\delta\Omega^+$  is defined as  $m\omega_0^2\zeta^2/2 + \delta\Omega$ . Integrating this density with respect to  $\varphi_1$  yields the probability density of  $\zeta$ , from which we can find its variance, *i.e.*, the mean square displacement. Apart from a multiplication constant, we can obtain the result of this integration by replacing  $\delta\Omega^+$  by the minimum of  $\delta\Omega^+$  for a given  $\zeta$  in the Boltzmann factor because the probability density considered here is a Gaussian distribution. We write  $\varphi_1^*$  for  $\varphi_1$  minimizing  $\delta\Omega^+$ , and thus  $\delta\Omega$ , for a given  $\zeta$ . The stationary condition of Eq. (B3) with respect to  $\varphi_1$  is found to be given by Eq. (55) with its lhs being put equal zero and Eq. (35) if  $\varphi^{(1)}$  and  $\zeta^{(1)}$  are respectively replaced by  $\varphi_1^*$  and  $\zeta$ . The condition is satisfied by

$$\varphi_1^*(\mathbf{r}) = -\zeta\varphi^{(0)'}(r) \cos\theta. \quad (\text{B4})$$

The time variable  $t$  need not be specified in this procedure. Replacing  $\varphi_1$  with  $\varphi_1^*$  in Eq. (B3), we find it to vanish. Thus, in this procedure, the mean square displacement remains the same as the first equation of Eq. (1). In this procedure, considering that the rhs of Eq. (B4) equals  $\varphi^{(0)}(r - \zeta \cos\theta) - \varphi^{(0)}(r)$  up to the order of  $\zeta$ , the profile of  $\varphi$  for a given  $\zeta$  is obtained by the translational shift of the profile of Fig. 1(a) and such a deformed adsorption layer as shown in Fig. 1(b) cannot be obtained. It is thus reasonable that no additional force due to the ambient near-criticality cannot be calculated in this incorrect procedure.

### Appendix C: Some details in the calculation

Substituting Eq. (40) into Eq. (6) gives

$$T_{10} = \frac{1}{\sqrt{2}r} \partial_r (r^2 R_{10}). \quad (\text{C1})$$

Picking up the terms with the order of  $\varepsilon$  from the  $r$ - and  $\theta$ -components of Eq. (9) and substituting Eqs. (19) and (40) into their Fourier transforms, we obtain

$$-i\omega\rho R_{10} = -\partial_r P_{10} - \varphi^{(0)} \partial_r Q_{10} \quad (\text{C2})$$

$$\text{and } \frac{-i\omega\rho r T_{10}}{\sqrt{2}} = -P_{10} - \varphi^{(0)} Q_{10}. \quad (\text{C3})$$

These three equations give Eq. (41).

Below,  $I_{3/2}$  and  $K_{3/2}$  represent modified Bessel functions. Using  $\tilde{s} \equiv s/s_c$  and  $\tilde{\sigma} \equiv \sigma/s_c$ , we define

$$\Gamma_{Gc}(s, \sigma) \equiv -w(s_c) K_{3/2}(\tilde{s}) K_{3/2}(\tilde{\sigma}) \tilde{\sigma}. \quad (\text{C4})$$

Here, we use

$$w(s_c) \equiv \frac{2e^{1/s_c} \{2s_c \cosh s_c^{-1} - (2s_c^2 + 1) \sinh s_c^{-1}\}}{\pi(1 + s_c)\kappa}, \quad (\text{C5})$$

which is the same as Eq. (4.10) of Ref. 15. The kernel used in Eq. (57) is defined as

$$\Gamma_G(s, \sigma) \equiv \begin{cases} \Gamma_{Gc}(s, \sigma) + K_{3/2}(\tilde{s}) I_{3/2}(\tilde{\sigma}) \tilde{\sigma} & \text{if } \sigma < s \\ \Gamma_{Gc}(s, \sigma) + I_{3/2}(\tilde{s}) K_{3/2}(\tilde{\sigma}) \tilde{\sigma} & \text{if } s \leq \sigma \end{cases}, \quad (\text{C6})$$

which is the same as Eq. (4.11) of Ref. 15. In deriving Eq. (57), we utilize the identity

$$K_{3/2} I'_{3/2} - I_{3/2}(s) K'_{3/2}(s) = s^{-1}, \quad (\text{C7})$$

and rewrite  $I_{3/2}$  and  $K_{3/2}$  in terms of elementary functions.

Equation (56) remains valid if  $\mathcal{Q}$  and  $\mathcal{G}$  are replaced by their respective outer solutions. Substituting (59) into the resultant equation gives

$$\mathcal{Q}_{\text{out}}(s) = -\frac{3\kappa}{s^2 \Xi(s)} \frac{d}{ds} \frac{\Xi(s)^2}{s^2} + \mathcal{O}(\Lambda^2). \quad (\text{C8})$$

Here, we note that the rhs of Eq. (56) with  $\mathcal{G}(s)$  replaced by  $\Xi(s)$  vanishes, which is found by substituting Eq. (12) into Eq. (29) and differentiating the result with respect to  $r$ . Taking the limit of  $s \rightarrow 1+$  of the derivative of Eq. (53) with respect to  $s$ , we use Eqs. (20), (21), and (62) to obtain

$$\mathcal{R}'(1+) = -3 - 2\Lambda^2 \left\{ -\frac{3}{\kappa} + \int_1^\infty ds \frac{\Xi(s)}{s} \mathcal{Q}_{\text{out}}(s) \right\}. \quad (\text{C9})$$

Substituting Eq. (C8) into Eq. (C9), we obtain Eq. (65) with the aid of the integration by parts.

Substituting Eq. (20) into Eq. (24) yields

$$D(s_c) = \frac{s_c^3}{(1 + s_c)^2} \left\{ \frac{E_8(s_c)}{s_c^2} + \frac{2E_9(s_c)}{s_c} + E_{10}(s_c) \right\}, \quad (\text{C10})$$

where we use

$$E_n(s_c) \equiv \frac{2^n e^{2/s_c}}{s_c^n} \int_{2/s_c}^{\infty} d\tau \tau^{-n} e^{-\tau} . \quad (\text{C11})$$

As  $s_c \rightarrow 0+$ , we have

$$E_n(s_c) \sim 1 - \frac{n}{2}s_c + \frac{n(n+1)}{4}s_c^2 + \mathcal{O}(s_c^3) . \quad (\text{C12})$$

Equations (C10) and (C12) give the asymptotic relation,

$$D(s_c) \sim s_c - 4s_c^2 + \mathcal{O}(s_c^3) \quad \text{as } s_c \rightarrow 0+ . \quad (\text{C13})$$

- 
- [1] B. Lukić, S. Jeney, C. Tischer, A. J. Kulik, L. Forró and E.-L. Florin, Phys. Rev. E **95**, 160601 (2005).
  - [2] T. Franosch, M. Grimm, M. Belushkin, F. M. Mor, G. Foffi, L. Forró, and S. Jeney, Nature **478**, 85 (2011).
  - [3] R. Huang, I. Chavez, K. M. Taute, B. Lukić, S. Jeney, M. Raizen, and E.-L. Florin, Nat. Phys. **7**, 576 (2011).
  - [4] M. Grimm, T. Franosch, and S. Jeney, Phys. Rev. E **86**, 021912 (2012).
  - [5] H. Lamb, *Hydrodynamics*, 6th ed., (Dover, New York, 1932), Sec. 92.
  - [6] J. W. Cahn, J. Chem. Phys. **66**, 3667 (1977).
  - [7] M. N. Binder, in *Phase Transition and Critical Phenomena VIII*, edited by C. Domb and J. L. Lebowitz, (Academic, London 1983).
  - [8] R. Holyst and A. Poniewierski, Phys. Rev. B **36**, 5628 (1987).
  - [9] R. Kubo, M. Toda, and N. Hashitsume, *Statistical Physics II*, (Springer, Berlin, 1991), Chap. 1.6.
  - [10] Why the energy is determined uniquely is discussed around Eq. (77) of Ref. 25.
  - [11] A. Furukawa, A. Gambassi, S. Dietrich, and H. Tanaka, Phys. Rev. Lett. **111**, 055701 (2013).
  - [12] Y. Fujitani, J. Phys. Soc. Jpn. **83**, 024401 (2014); **83**, 108001 (2014) [erratum].
  - [13] Y. Fujitani, J. Phys. Soc. Jpn. **83**, 084401 (2014).
  - [14] Y. Fujitani, J. Phys. Soc. Jpn. **82**, 124601 (2013); **83**, 088001 (2014) [erratum].
  - [15] R. Okamoto, Y. Fujitani, and S. Komura, J. Phys. Soc. Jpn. **82**, 084003 (2013).
  - [16] S. Yabunaka, R. Okamoto, and A. Onuki, arXiv:1412.7398v2 [condmat.soft].
  - [17] A. Onuki, *Phase Transition Dynamics*, (Cambridge University Press, Cambridge, England, 2002), Chaps. 4 and 6.
  - [18] K. Kawasaki, Ann. Phys. (N. Y.) **61**, 1 (1970).
  - [19] P. C. Hohenberg and B. I. Halperin, Rev. Mod. Phys. **49**, 435 (1977).
  - [20] A. J. Bray and M. A. Moore, J. Phys. A: Math. Gen. **10**, 1927 (1977).
  - [21] W. H. Diehl, in *Phase Transition and Critical Phenomena X*, edited by C. Domb and J. L. Lebowitz, (Academic, London 1986).
  - [22] T. W. Burkhardt and H. W. Diehl, Phys. Rev. B **50**, 3894 (1994).
  - [23] W. H. Diehl, Int. J. Mod. Phys. B **11**, 3503 (1997).
  - [24] C. M. Bender and S. A. Orszag, *Advanced Mathematical Methods for Scientists and Engineers*, (Springer, New York, 1999), Chaps. 1.5 and 9.2.
  - [25] Y. Fujitani, Phys. Rev. E **91** 042402 (2015).
  - [26] P. G. de Gennes, *Scaling Concepts in Polymer Physics*, (Cornell Univ Press, Ithaca, 1979), Sec. III. 1. 3.
  - [27] J. O. Indekeu, P. J. Upton, and J. M. Yeomans, Phys. Rev. Lett. **61**, 2221 (1988).
  - [28] P. J. Upton, J. O. Indekeu, and J. M. Yeomans, Phys. Rev. B **40**, 666 (1989).
  - [29] A. J. Liu and M. E. Fisher, Phys. Rev. A **40**, 7202 (1989).
  - [30] A. Hanke and S. Dietrich, Phys. Rev. E **59**, 5081 (1999).
  - [31] Substituting Eq. (C8) into the lhs of Eq. (61) yields the rhs. This is an alternative way of deriving Eq. (61).
  - [32] I. Iwanowski, K. Leluk, M. Rudowski, and U. Kaatz, J. Phys. Chem. A **110**, 4313 (2006).
  - [33] J. S. Rowlinson and B. Widom, *Molecular Theory of Capillarity*, (Clarendon Press, UK, 1982), Chapters 3, 4.6, and 9.1-2.
  - [34] C. I. Poser and I. C. Sanchez, Macromolecules **14**, 361 (1981).
  - [35] B. S. Carley, L. E. Scriven, and H. T. Davis, AIChE J. **26** 705 (1980).
  - [36] P. M. W. Cornelisse, C. J. Peters and J. de Swaan Arons, Fluid Phase Equilib. **117**, 312 (1996).
  - [37] D. Riveline, J. Nanobiotechnol. **11**, 51 (2012).
  - [38] R. Okamoto and A. Onuki, J. Chem. Phys. **136**, 114704 (2012).
  - [39] R. Okamoto and A. Onuki, Phys. Rev. E **88**, 022309 (2013).
  - [40] D. F. Litim, Phys. Rev. D, **64** 105007 (2001); J. Berges, arXiv:hep-ph/9902419v1.
  - [41] Y. Fujitani, arXiv:1510.02870 [condmat.soft]
  - [42] J. Rudnick and D. Jasnow, Phys. Rev. Lett **48**, 1059 (1983).
  - [43] W. H. Diehl, Ber. Bunsenges, Phys. Chem. **98**, 466 (1994).
  - [44] M. Smock, H. W. Diehl, and D. P. Landau, Ber. Bunsenges, Phys. Chem. **98**, 486 (1994).
  - [45] H. W. Diehl and M. Smock, Phys. Rev. B **47**, 5841 (1993); **48**, 6740 (1993) [erratum].